AAME

RSA(EXT) 46

January 1994

# Determination of photon fluence spectra from the NPL Mobaltron $^{60}$Co unit

D R Shipley and S Duane
Division of Radiation Science and Acoustics
National Physical Laboratory
Queens Road
Teddington
Middlesex
United Kingdom
TW11 0LW

## ABSTRACT

Absorbed dose to water calibrations of secondary standard hospital dosemeters are carried out at NPL in both X-radiation from 4 MV to 19 MV and in $^{60}$Co $\gamma$-radiation. Measurements are performed using the primary standard graphite calorimeter and by inserting the secondary standard and working standard chambers at a reference depth in either a water or graphite phantom. Details of the dose distributions and the responses of these chambers in each phantom for the NPL $^{60}$Co radiation quality are, however, unknown. A knowledge of the photon fluence spectra produced by the NPL $^{60}$Co unit is therefore required to enable this analysis to be carried out. This report describes the work that was undertaken to determine the photon fluence spectra incident on the front face of the water and graphite phantoms under standard measurement conditions. The spectra were validated by comparing calculated tissue-phantom ratios with recent experimental values.

The calculated TPR values were found to agree with measurements to within 1-2$\sigma$ (total uncertainty), and also with independent estimates obtained using the program AVERMV. The observed discrepancies were primarily systematic in nature with the largest source of uncertainty being the change in beam quality, and hence chamber calibration factor, with depth in the phantom.

ISSN 0955-9655

National Physical Laboratory
Teddington, Middlesex, UK, TW11 0LW



Approved on behalf of Chief Executive, NPL,
by Dr P Christmas, Acting Head, Division of Radiation Science and Acoustics.

CONTENTS



ILLUSTRATIONS



TABLES

# 1 INTRODUCTION

The National Physical Laboratory (NPL) provides a High Energy Absorbed Dose Service, based on a primary standard graphite calorimeter, for the calibration of hospital secondary standard dosemeters in terms of absorbed dose to water[1]. The calibrations are performed for high energy X-radiation over the energy range 4 to 19 MV and for $^{60}$Co $\gamma$-radiation. The latter radiation quality was introduced to allow intercomparisons with BIPM and the other national standardising laboratories which have also developed absorbed dose standards in $^{60}$Co $\gamma$-radiation.

The $^{60}$Co unit used at the NPL is a TEM Mobaltron which has the source slug mounted on a rotating wheel inside the lead shielding. A continuously variable collimator is attached to the front of the unit giving square and rectangular fields in a horizontal beam. Measurements with secondary standard and working standard ionization chambers are carried out by inserting the chambers at a reference depth in either a water or a graphite phantom. To enable the future analysis of the response of these chambers and to determine the dose distributions in each phantom, a knowledge of the photon fluence spectra produced by the Mobaltron unit is required.

The first part of this report therefore describes the work undertaken to determine the photon fluence spectra produced by the NPL Mobaltron unit incident on the front face of the water and graphite phantoms under standard measurement conditions. Monte Carlo techniques were used throughout based on the EGS4[(1)] code system[2]. The methods used to validate the spectra are described in the second part of the report. Here, calculated tissue-phantom ratios for these spectra are compared with recent experimental values and any discrepancies are discussed.

# 2 CONSTRUCTION OF THE NPL MOBALTRON UNIT

The construction of the source housing and collimator system of the Mobaltron unit is shown in Figure 1. The source consists of two stainless steel modules, one loaded behind the other, in a source slug, each containing discs of Cobalt metal (17.0 mm in diameter and 1.1 mm thick). The module at the front of the source slug contains 10 discs with a total estimated activity of 89.2 TBq (as of 1 March 1993). The rear module contains 8 discs with an estimated activity of 39.6 TBq. The slug itself is located on a rotating drum and is aligned with the beam axis by remote control.

A tungsten-alloy conical collimator is present immediately in front of the source. This has a small aperture approximately half-way along its length containing a beam-defining light source. Above this aperture, is a small glass mirror, fixed in place with a brass ring at 45 degrees to the beam axis.

Attached to the front of the Mobaltron head is the continuously variable collimator which defines the beam size. It consists of four adjustable tungsten apertures of slightly different size which give a beam rectangular in cross-section at the front face of the phantom. Two aperture settings are used most often. For ion chamber measurements at 5 cm depth in a water phantom at a focal distance of 95 cm (measured from the front face of the source), an aperture setting of 6.0 × 6.0 is used. This gives a field size of 10 cm × 10 cm at the chamber depth. For measurements at 3.2 cm depth in a graphite phantom at a focal distance of 70 cm, an aperture setting of 7.8 × 7.8 is used, which also gives a 10 cm × 10 cm field size at the chamber depth.

---

(1) Electron-Gamma Shower version 4.

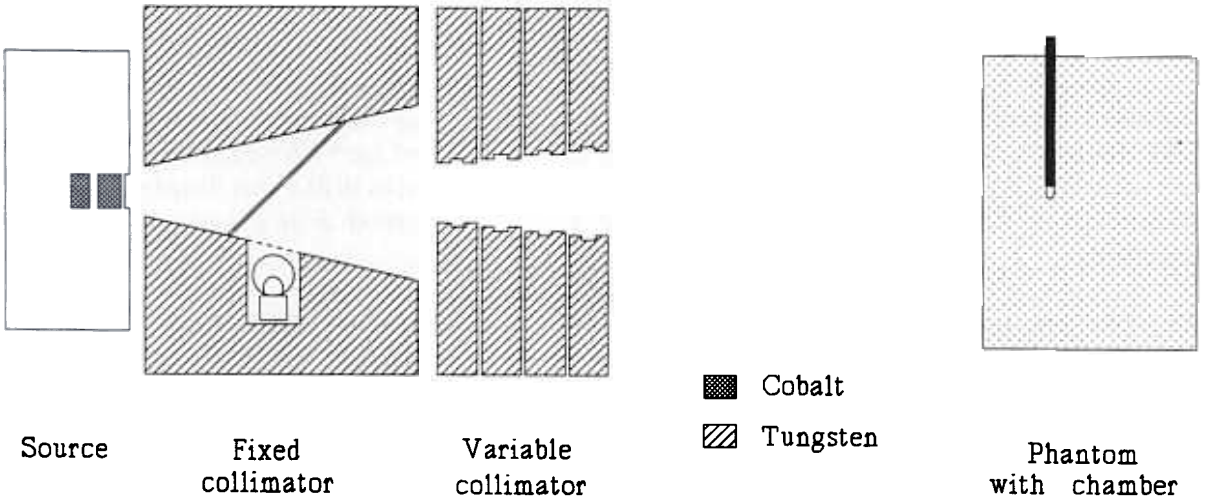


Figure 1 Schematic diagram showing the construction of the source housing and collimator system of the NPL Mobaltron $^{60}$Co unit.

## 3 CALCULATION OF THE PHOTON FLUENCE SPECTRUM

### 3.1 THE EGS4 CODE SYSTEM

Most of the calculations described in this report were carried out using the EGS4 code system with the PRESTA[(2)] electron transport algorithm[3]. These codes form a general purpose package for the Monte Carlo simulation of the coupled transport of electrons and photons in an arbitrary geometry for particles with energies ranging from a few keV to several TeV. The package, used in conjunction with a user-written code, calculates the development of an electron-photon cascade from a single incident electron or photon, and transports each and every particle through the geometry until it reaches a predefined energy cutoff or discard boundary. Electron-photon transport can be simulated in any of 100 elements or mixture of these elements, or any compound. The associated package PEGS4[(3)], documented by Nelson et al.[2], is used to generate datasets of the required materials for subsequent use by EGS4.

### 3.2 METHOD OF CALCULATION

An EGS4 user code MOBALTRN (Version 2.20) was developed to calculate the photon fluence spectra incident on the front face of the water and graphite phantoms. This code simulates the passage of electrons and photons through the Mobaltron unit and stores the full phase space information (that is, the energy, position and direction cosines) of those photons that reach the scoring plane at a specified distance from the front face of the source. For the photon fluence incident on the water phantom, the scoring plane was placed at 90.0 cm from the source. For the graphite phantom, the scoring plane was placed at 66.8 cm from the source. The associated FORTRAN77 program PLOTFL (Version 1.01) was used to calculate the photon fluence spectrum from the stored photon data.

The simulation geometry used to represent the Mobaltron unit in MOBALTRN matches the actual construction quite closely. There are only two major differences which may affect the photon spectrum (and which greatly reduce the complexity of the code). Firstly, the small aperture containing the light source in one side of the conical collimator has been replaced

---

(2) Parameter Reduced Electron-Step Transport Algorithm.

(3) Preprocessor for EGS4.

with a planar aperture which extends all the way around the collimator surface (perpendicular to the beam axis). Secondly, the beam defining mirror fixed at 45 degrees to the beam axis has been replaced with one perpendicular to the axis, either immediately in front of or behind the aperture. The simulations have shown, however, that there is in practice no significant difference in the calculated photon fluence spectra with the mirror placed in front of or behind the aperture, or with the planar aperture present or absent. The beam defining mirror was therefore placed in the rear position, nearer to the source, and the planar aperture was removed for all fluence spectra calculations in this work, since this setup most closely matches the actual setup.

The coding for the simulation geometry and the material definitions were checked using the MORTRAN3 program MGTEST3 (Version 3). This code first places point sources at random in each geometric region and then stores the coordinates of the point of intersection of a randomly-directed 'ray' with the nearest boundary. The outline of each region is then revealed when the points are plotted with an appropriate graphics package. The points from regions containing the same material can also be grouped together to enable the distribution of a given material throughout the geometry to be verified.

The datasets required by EGS4 for all the materials in the simulation geometry were generated using PEGS4. In particular, the dataset for the source material in each module was based on the actual composition as of 1 March 1993 (estimated from the measured activity and half-life).

The EGS4 transport parameters were set to the following values for all regions in the geometry. The minimum (total) electron energy required for explicit δ-ray production, AE, was set to 0.521 MeV, and the minimum (total) energy for electron transport, ECUT, was set to 2.511 MeV. AP and PCUT, the photon equivalents of AE and ECUT, were set to 0.010 MeV and 0.040 MeV respectively. With these cutoffs, there is no electron transport in the simulations since the electrons are discarded immediately after they are produced. This has no significant effect on the photon fluence spectrum and greatly reduces the computation time per initial decay. A photon transport cutoff of 0.040 MeV was chosen since this represents the lowest photon energy expected in the fluence spectrum, an expectation borne out by the results.

The photon fluence calculations were performed on an Elonex PC-466 PC system using Lahey F77L-EM/32 Fortran (Version 5.01). With 50.0 M initial photon decays (at a rate of 3.5 M decays per hour), approximately 86600 photons reach the scoring plane with an aperture setting of 7.8 × 7.8 and 51400 reach the scoring plane with an aperture setting of 6.0 × 6.0.

## 3.3 RESULTS

The calculated photon fluence and photon energy fluence spectra for the Mobaltron unit at 90 cm from the source (with an aperture setting of 6.0 × 6.0) is shown in Figure 2 after 50.02 M decays. Of the 51400 photons that reach the scoring plane, approximately 50200 actually strike the front face of the water phantom (26.5 cm × 26.5 cm in size). The two emission lines at 1.17 MeV and 1.33 MeV account for approximately 73% of the total energy fluence. A third line at approximately 510 keV is also visible above the scatter background. This line is due to annihilation photons being produced in the shielding immediately surrounding the source modules (confirmed using a graphics package to display individual histories). A compton edge at around 210 keV can also be seen due to primary photons back-scattering from the walls of the source modules.

Figure 3 shows the calculated fluence spectra at 66.8 cm from the source (with an aperture setting of 7.8 × 7.8) after 50.01 M decays. Here approximately 82500 photons strike the front face of the graphite phantom (17.2 cm × 17.2 cm in size), 60% more than with the water

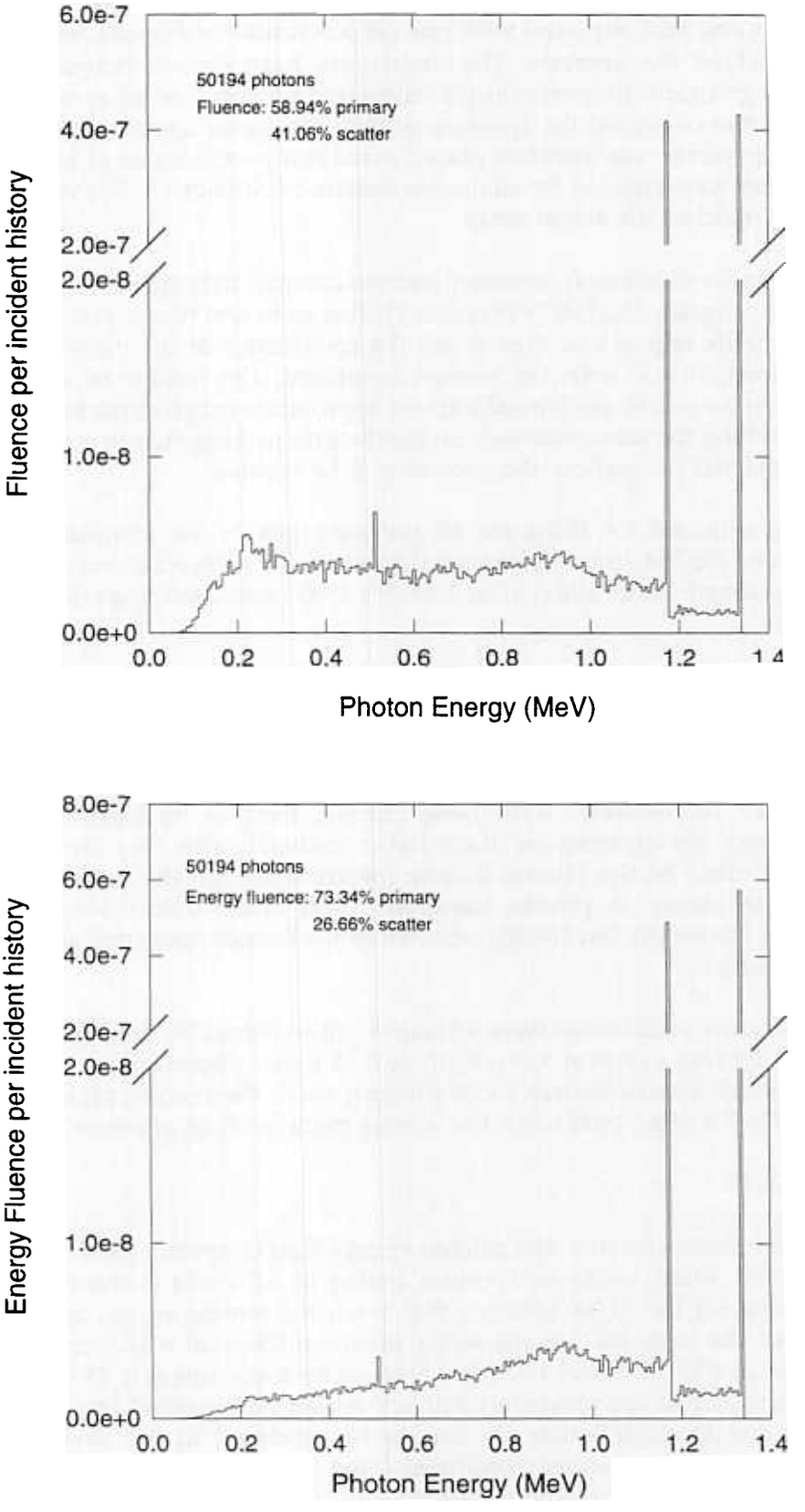


Figure 2 Calculated photon fluence and photon energy fluence spectra produced by the Mobaltron unit with an aperture setting of 6.0 × 6.0 incident on the front face of the water phantom. The phantom is placed at a distance of 90 cm from the front face of the source.

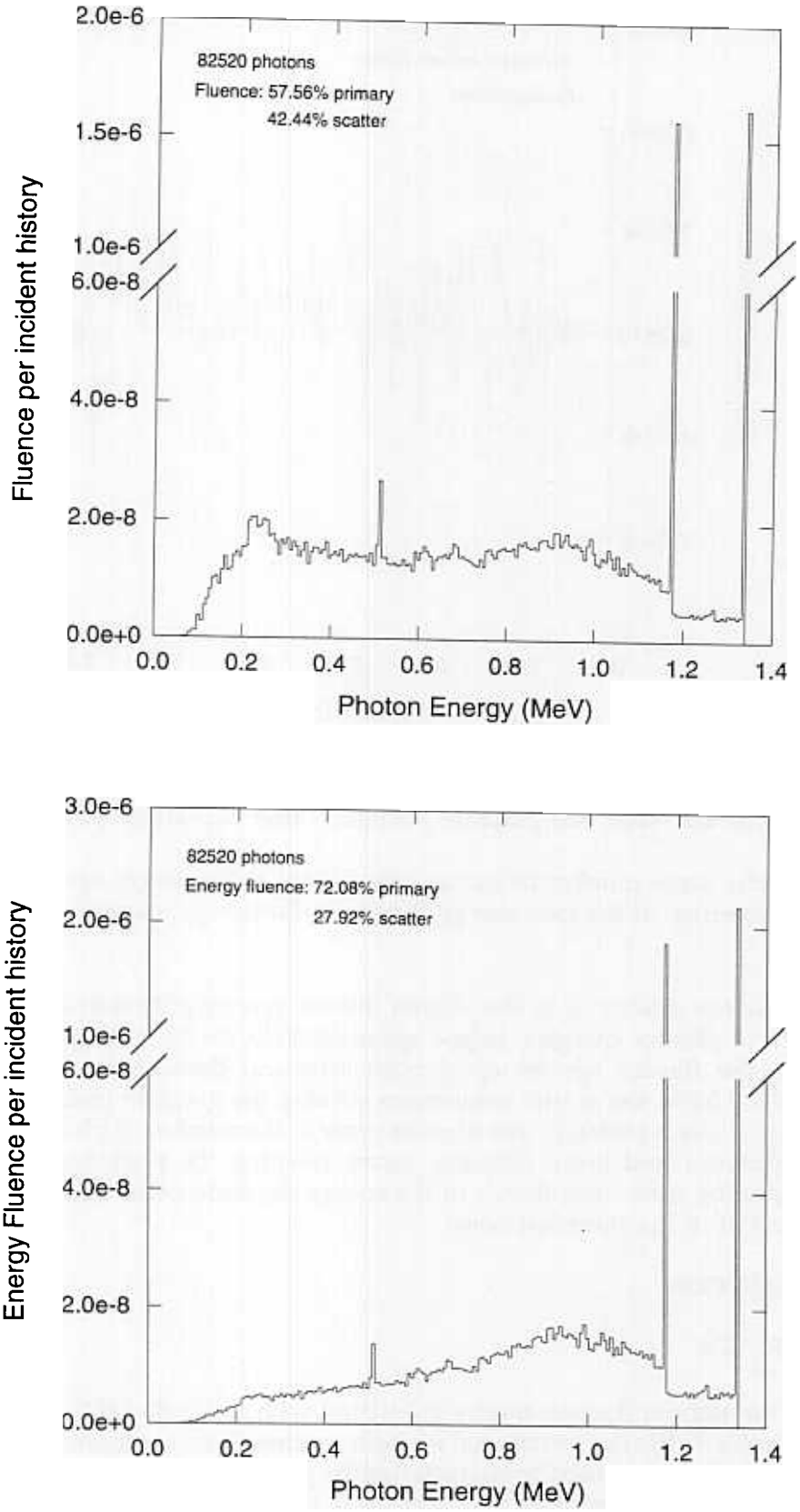


Figure 3 Calculated photon fluence and photon energy fluence spectra produced by the Mobaltron unit with an aperture setting of 7.8 × 7.8 incident on the front face of the graphite phantom. The phantom is placed at a distance of 66.8 cm from the front face of the source.

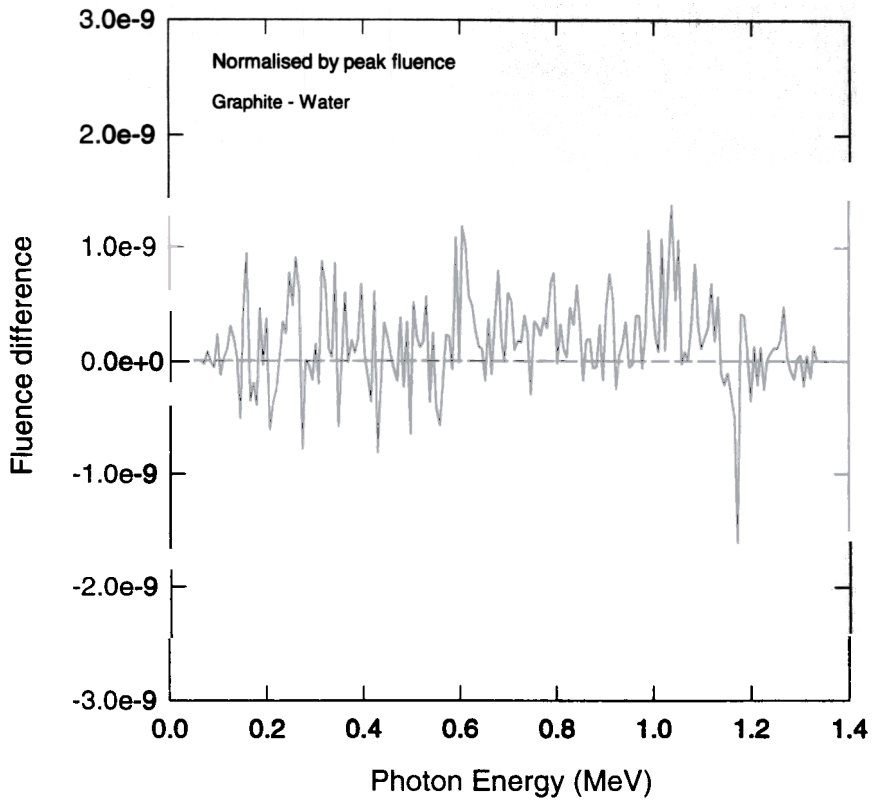


Figure 4 Difference in the calculated photon fluence spectra incident on the front face of the water and graphite phantoms after normalising by the peak fluence.

phantom for the same number of initial decays (due to the larger aperture setting being used). The proportion of the total energy fluence in the two primary lines, however, is very similar.

Figure 4 shows the difference in the photon fluence spectra after normalising by the peak fluence. At low photon energies, below approximately 0.6 MeV, there appears to be no difference in the fluence spectra apart from statistical fluctuations. However, between 0.6 MeV and 1.2 MeV, the scatter component striking the graphite phantom appears to be slightly greater. This is probably due to an increase in the number of photons scattered from the fixed collimator and beam defining mirror reaching the phantom due to the larger aperture size being used. Any details of the energy dependence of this scatter component, however, are lost in the statistical noise.

## 4 VALIDATION

### 4.1 OVERVIEW

To validate the photon fluence spectra calculated with the code MOBALTRN, the tissue-phantom ratio (or TPR) was determined for each spectrum and compared with experimental values. The TPR(20/10) is used to characterise the photon beam and is defined as the ratio of absorbed dose on the beam axis at 20 cm and 10 cm depths in a large water phantom, with a constant focal distance to the point of measurement, and with a 10 cm × 10 cm field size in the plane of measurement. The TPR(10/5) is also of interest and is the ratio of absorbed dose at 10 cm and 5 cm depths in water under the same conditions.

The TPR(20/10) and TPR(10/5) were measured on the Mobaltron unit, at focal distances of

70 cm and 95 cm, using an NE 2561 ionization chamber in a waterproof perspex sheath placed in a 30 cm cube water phantom. The ratio of measured ionization currents at the different depths was taken to be equal to the ratio of absorbed doses. No account was taken of any change in the chamber calibration factor which may be appropriate to the different depths in the phantom.

## 4.2 METHOD OF CALCULATION

The EGS4 user code DOSRZ (NPL Version 1.0) was used with EGS4/PRESTA to calculate the TPR values for the Mobaltron fluence spectra at 70 cm and 95 cm from the source. This code calculates the dose deposited (per incident particle) in selected regions in a cylindrical-planar geometry. The source routines used with DOSRZ were modified to allow the list of photon parameters generated by MOBALTRN to be used in the TPR calculations. This list was re-read many times in each calculation.

The simulation geometries used to calculate the dose deposited on the beam axis at 5 cm, 10 cm and 20 cm depth in a water phantom, at both 70 cm and 95 cm from the source, are shown in Figure 5. Here, the cubic water phantom has been replaced with a cylindrical phantom of the same length and frontal area (radius 14.95 cm). Simulations have shown that this change has an insignificant effect ($<1\sigma$) on the TPR since the frontal area is much greater than the 10 cm × 10 cm field size used. The dose was scored in three 1 cm thick slabs and three 1 cm radius concentric cylinders (giving 9 scoring regions in all) centred at the required depth in the phantom (as shown).

Since the size of the scoring regions used in the calculations are small compared to the field size at each depth, and the number of incident histories used are typically 3 orders of magnitude greater than the number of distinct photons in the incident spectrum (generated by MOBALTRN), there may be some systematic dependency of the dose value on individual photons in the spectrum. One way to reduce such a dependency would be to significantly increase the number of photons in the incident spectrum. However, this would require a large amount of computation time since the simulation of the Mobaltron unit is very inefficient, with only ~0.1% of initial photon decays actually reaching the scoring plane. The preferred option, which was chosen in this work, is to use the *same* incident photon spectrum (at each focal distance) to calculate the absorbed dose at the different depths in the water phantom. The advantage of this method is that the dose values are correlated and any dependency of these individual values on the incident spectrum should largely cancel when evaluating the TPR.

To enable the calculation of correlated dose values at a focal distance of 95 cm, the photon fluence spectrum at 75 cm from the source was first determined using MOBALTRN, with an aperture setting of 6.0 × 6.0. This photon data was then used to calculate the absorbed dose at 5 cm depth in a water phantom by inserting a 15 cm thick slab of air in front of the phantom (see Figure 5). To calculate the dose at 10 cm depth in water, a 10 cm thick air slab was used. No air slab was required for the dose calculation at 20 cm depth. At a focal distance of 70 cm, the photon fluence spectrum at 50 cm from the source was first determined (with an aperture setting of 7.8 × 7.8). The dose values at each depth were then determined using the same air slab thicknesses as before. The TPR(20/10) (at 70 cm and 95 cm) and TPR(10/5) (at 95 cm only) were obtained by first calculating dose ratios for the nine corresponding scoring regions at the required depths in the phantom and then taking the mean of these ratios (weighted by the volume of each region).

The EGS4 transport parameters were set to the following values for each dose calculation. The minimum (total) electron energy for δ-ray production, AE, was set to 0.700 MeV, and the minimum energy for electron transport, ECUT, was set to 1.311 MeV. The corresponding photon cutoffs AP and PCUT were both set to 0.010 MeV. ECUT was chosen so that the

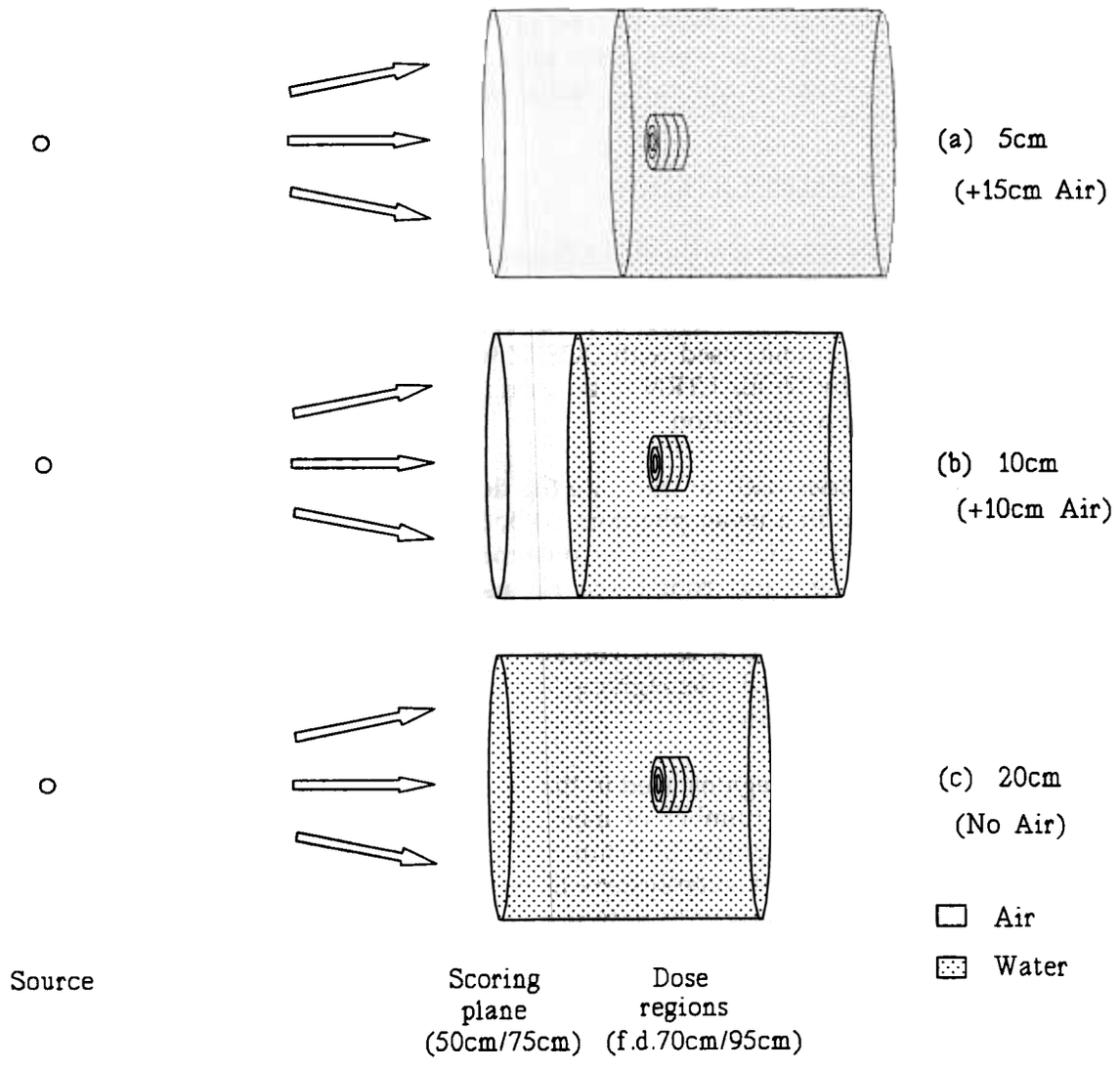


Figure 5 Simulation geometries used to calculate the dose deposited at, (a) 5 cm, (b) 10 cm, and (c) 20 cm, in a water phantom at focal distances of 70 cm and 95 cm from the source.

CSDA[4] range of an electron of this energy in the smallest scoring region is approximately one-third the minimum dimension of this region (a 'rule of thumb'). The PRESTA routines were also invoked to improve the efficiency of electron transport in water. The dose calculations were performed on a HP 9000/720 workstation using the UNIX version of EGS4 (Version 2.0) and HP FORTRAN/9000 (Version 9.0). With these parameters, approximately 60.0 M incident photons were required at each depth to calculate the dose in each scoring region to a statistical uncertainty of 0.5% or better (at 1σ).

## 4.3 RESULTS

The calculated and experimental TPR values at focal distances of 70 cm and 95 cm from the Mobaltron source, with their estimated statistical uncertainties at the 1σ level, are given in Table I. An estimate of the possible range of values for TPR(20/10) calculated using the code AVERMV, developed by Andreo and Nahum[4], are also given for comparison. AVERMV is

[4]The range of a charged particle in the continuous slowing down approximation.

Table I Comparison of calculated and experimental TPR values at different focal distances from the source. The statistical uncertainties are given at the 1σ level.

| | Focal distance (cm) | Calculation | Experiment | AVERMV |
|---|---|---|---|---|
| TPR(20/10) | 95.0 | 0.5700 ± 0.0004 | 0.5716 ± 0.0002 | 0.5686–0.5725 |
| TPR(10/5) | 95.0 | 0.7901 ± 0.0006 | 0.7941 ± 0.0003 | - |
| TPR(20/10) | 70.0 | 0.5616 ± 0.0004 | 0.5676 ± 0.0004 | 0.5638–0.5659 |

a code that calculates depth dose curves in water for bremsstrahlung spectra using monoenergetic data for circular parallel beams generated using Monte Carlo techniques. In particular, the ratio of absorbed doses at 10 cm and 20 cm depth in water is quoted. This code can therefore be used to obtain an independent estimate for TPR(20/10) for the calculated Mobaltron fluence spectra.

At a focal distance of 95 cm, the agreement between calculated and experimental TPR's is better than 0.5%, whereas, at a focal distance of 70 cm, the calculated value for TPR(20/10) is 1.2% lower than the corresponding experimental value. The discrepancies between calculation and experiment are significantly greater than the estimated statistical uncertainties quoted in the table and are most likely due to other systematic effects not fully accounted for in the calculations (see Section 5).

The calculated value for TPR(20/10) also lies inside the range estimated using AVERMV at 95 cm, although it is 0.4% smaller than the lower limit of the range at 70 cm. The validity of the AVERMV results is open to some question since these results are based on Monte Carlo calculations using parallel photon beams that are circular in cross-section. The photon beams from the Mobaltron unit used in the TPR calculations, however, are diverging and square in cross-section. There is therefore some uncertainty in the beam radius that should be used with AVERMV to represent the Mobaltron beam. (In this case, the beam radius that gives the same cross-sectional area as the field size used in the TPR measurements was chosen[5]). The TPR values obtained using AVERMV were also observed to be quite sensitive to the beam radius, increasing by approximately 0.2% for each millimetre increase in beam radius.

## 5 DISCUSSION AND UNCERTAINTIES

It can be seen from the results in Table I that the discrepancies between calculation and experiment are significantly greater than the quoted statistical uncertainties. These discrepancies are therefore presumed to be systematic in nature and will be discussed in more detail in this section.

There are several possible sources of systematic uncertainty in the calculation of the Mobaltron fluence spectra and their corresponding TPR values. One source is the dependence of the calculated dose at depth in a water phantom on individual photons in the spectrum, as discussed in Section 4.2. However, in the calculation of TPR, this dependence and associated systematic uncertainty is expected to be much reduced when correlated dose values are used.

The calculated TPR was found to be quite sensitive to the amount of scattered radiation in

the incident photon spectrum. The TPR(20/10) calculated at 70 cm from the source increases by 3.4% to 0.5810 ± 0.0004 (1σ) when only the *primary* photon spectrum is taken, that is, 2.4% greater than the corresponding experimental value. Thus the discrepancy in TPR values at 70 cm focal distance could be explained by the scatter component in the calculated Mobaltron fluence spectra being overestimated by ~40%. This is unlikely, however, since the agreement in TPR values at 95 cm focal distance is much better (~0.3%). One should note that a somewhat greater scatter component is expected in the photon fluence spectrum at 70 cm than at 95 cm, since a larger aperture size is being used, but probably not enough to completely account for the observed discrepancies (see Section 3.3).

The statistical fluctuations in the fluence values in each energy bin in the incident spectrum (i.e. the spectrum 'noise') may also affect the TPR. Subsequent calculations have shown, however, that the TPR derived from two independently calculated Mobaltron fluence spectra, generated under the same conditions, agree to within 0.1% (i.e. 1-2σ).

The TPR calculations do not take account of radiation scattered from the surrounding room, and, in particular, photons back-scattered from the large lead beam-stop approximately 2 metres from the source along the beam axis. The mean free path of these back-scattered photons may be sufficiently large to affect the absorbed dose at 20 cm depth in the water phantom (which is only ~10 cm from the back face of the phantom). However, TPR calculations with the beam-stop present, and experimental measurements with an additional lead wall placed close to the back of the water phantom, showed that back-scattered radiation does not significantly affect the TPR.

The largest systematic uncertainty is thought to be associated with the experimental measurements of TPR. These measurements use an NE 2561 ionization chamber that has been calibrated at 5 cm depth in a water phantom, the standard depth used in the absorbed dose to water calibration service. For all the measurements carried out in this work, the *same* chamber calibration factor has been used with no account taken of any change in this factor at different depths in the water phantom. The beam quality, in fact, increases with depth in the water phantom and thus one would expect the chamber calibration factor to decrease accordingly. This would reduce the measured TPR values and hence reduce the observed discrepancies between calculation and experiment. Unfortunately, it is difficult to estimate this change in TPR since no information is yet available on the variation of calibration factor for an NE 2561 chamber with depth in a water phantom.

The total systematic uncertainty in the calculated TPR values primarily due to the scatter component in the Mobaltron fluence spectra being overestimated is thought to be 0.1% (1σ). The total systematic uncertainty in the experimental TPR values due to the change in chamber calibration factor not being accounted for in the measurements is estimated to be no more than 0.5% (1σ). Thus the total uncertainty (statistical and systematic taken in quadrature) in the calculated and experimental TPR values is 0.13% and 0.51% respectively at the 1σ level.

## 6 CONCLUSIONS

The calculated TPR values agree with their corresponding experimental values to within 1-2σ (total uncertainty) suggesting that the techniques used in this work to determine the photon fluence spectra produced by the Mobaltron unit are reliable. The calculated values also show agreement with independent estimates determined using AVERMV even though these results are based on Monte Carlo simulations using parallel photon beams that are circular in cross-section.

The observed discrepancies between calculated and experimental TPR values are presumed to be systematic in nature, partly due to an overestimate of the scatter component in the Mobaltron fluence spectra (probably caused by the simplifications in the simulation

geometry), but primarily due to the change in beam quality with depth in the phantom not being accounted for in the experimental measurements. This change in beam quality with depth will be investigated in more detail in a future project.

## 7 ACKNOWLEDGEMENTS

The authors would like to thank Karen Rosser and Amanda Barnicoat for carrying out the experimental measurements of TPR, and Colin Brend for obtaining all the relevant details relating to the construction of the source slug and housing of the NPL Mobaltron unit.

## 8 REFERENCES

1 BURNS, J.E. and DALE, J.W.G. Conversion of absorbed-dose calibration from graphite into water. *NPL Report RS(EXT) 7*, April 1990.

2 NELSON, W.R., HIRAYAMA, H. and ROGERS, D.W.O. The EGS4 code system. *Report SLAC-265*, Stanford Linear Accelerator Center, Stanford, CA 94305, 1985.

3 BIELAJEW, A.F. and ROGER, D.W.O. PRESTA—the Parameter Reduced Electron-Step Transport Algorithm for electron Monte Carlo transport. *Nucl. Instr. and Meth.*, 1987, **B18**, 165–181.

4 NAHUM, A.E. Private communication. 1993.

5 BJR. Central axis depth dose data for use in radiotherapy. *Supplement 17 to British Journal of Radiology*, British Institute of Radiology, London, 1983.